Carbohydrate Research 405 (2015) 66–69

Contents lists available at ScienceDirect

Carbohydrate Research

journal homepage: www.elsevier.com/locate/carres

Fluorous-based carbohydrate Quartz Crystal Microbalance

Lei Chen, Pengfei Sun, Guosong Chen *

The State Key Laboratory of Molecular Engineering of Polymers, Department of Macromolecular Science, Fudan University, Shanghai 200433, China

ARTICLE INFO

Article history:
Received 18 May 2014
Received in revised form 28 July 2014
Accepted 30 July 2014
Available online 7 August 2014

Keywords:
Carbohydrate
Fluorous
QCM
Lectin
CCI

ABSTRACT

Fluorous chemistry has brought many applications from catalysis to separation science, from supramolecular materials to analytical chemistry. However, fluorous-based Quartz Crystal Microbalance (QCM) has not been reported so far. In the current paper, fluorous interaction has been firstly utilized in QCM, and carbohydrate–protein interaction and carbohydrate–carbohydrate interaction have been detected afterward.

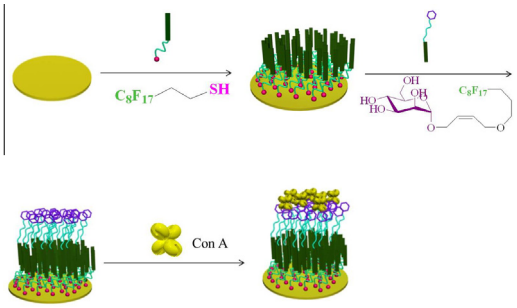

1. Introduction

Gladysz, Horváth and Curran introduced fluorous chemistry at the end of last century.[1,2] As a kind of non-covalent interaction, fluorous interaction is based on the specific affinity between fluorous compounds (organic compounds contain C_nF_{2n+1}-group (n = 6–8), fluorous tail). The interaction is quite unique and independent to the well-known hydrophobic and hydrophilic ones, which brings many applications in different fields. For example, separation of fluorous and non-fluorous compounds can be easily achieved via fluorous solid phase extraction (F-SPE)[3], in which separation was achieved via the fluorous-modified silica gel. In 2005, the interaction was first introduced to small molecular microarray by Pohl et al.[4] Fluorous-modified carbohydrates were immobilized to glass surface via fluorous interaction and their binding ability to lectins was measured. Later on, various small molecules were introduced to glass surface via fluorous interaction aiming at microarray measurements.[5]

Considering the success of fluorous microarray, expanding the fluorous interaction to other analytical instruments is of great importance. Quartz Crystal Microbalance (QCM) is a mass sensor based on the piezoelectric properties of quartz crystals with many applications in both scientific research and industry.[6] Recently, QCM with dissipation monitoring (QCM-D) technique was developed as an extension, which simultaneously measures changes in the induced energy dissipation (ΔD) and the frequency (ΔF), and enables a label-free detection and analysis of bio-recognition events in real-time.[7] Comparing to microarray, QCM has its own pros and cons. Currently high throughput screening could not be easily achieved, which might be the major drawback of QCM. However, by using QCM, interactions between protein and ligand can be easily measured without any fluorescent labeling and the whole binding process can be monitored in situ. These two

* Corresponding author.
E-mail address: guosong@fudan.edu.cn (G. Chen).

http://dx.doi.org/10.1016/j.carres.2014.07.023
0008-6215/

advantages make QCM more suitable to measure some complicated interactions with the analytes of high molecular weight. Furthermore, in a typical QCM-D measurement, energy dissipation (ΔD) could provide a viscoelastic parameter related to the properties of the propagation material.[8]

Thus it is quite valuable to combine fluorous interaction with QCM-D, which in fact has never been reported before. In this paper, the first example of QCM based on fluorous interaction will be demonstrated. Carbohydrate–protein interaction and carbohydrate–carbohydrate interaction (CCI) will be detected on fluorous surface. Under the help of ΔD, non-specific interaction can be differentiated from the specific ones. Thus the method reported in this paper has a promising future to be developed into a general detection method for various interactions.

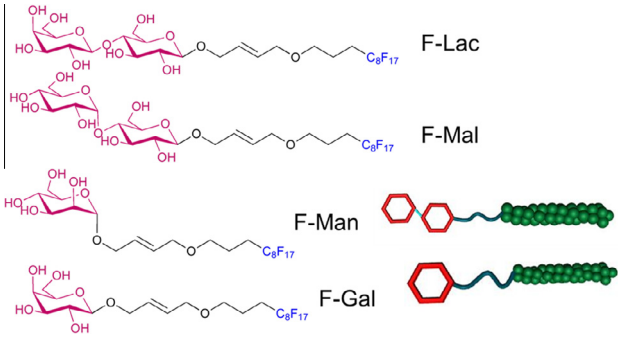

Scheme 1. Chemical structures of fluorous sugars used in this study.

2. Results and discussion

Typically, pre-cleaned gold chip was first immersed in an isopropanol solution of 1*H*,1*H*,2*H*,2*H*-perfluorodecyl thiol (F-SH, 17% v:v). After 24 h, the chip was washed with pure isopropanol twice then water, and dried under nitrogen. The successful immobilization of fluorodecanethiol was proved by contact angle measurement. As shown in Figure 1a and b, the contact angles of gold surface before and after immobilization of fluorodecanethiol are 63° ± 2° and 105° ± 1°, respectively. This transformation from hydrophilic to hydrophobic supports the successful modification of F-SH on gold surface.

The next step is to coat fluorous-modified sugars (F-sugars) to the fluorous surface of gold chips. Four different F-sugars, including **F-Lac**, **F-Mal**, **F-Gal**, and **F-Man** (Scheme 1) are prepared according to the reported synthetic procedures.[9] The coating step looks straightforward at first, because F-sugars were successfully loaded to fluorous-coated glass slide in microarray assays. In microarray experiments, F-sugars were first dissolved in the mixture of DMF/MeOH/water, then the sample was loaded to the fluorous glass surface via automated pin in microliter scale. The spots finally obtained on glass surface were in the size of ca 100 μm, which was very easy to be dried and immobilized. No further washing is necessary because the amount of F-sugars on surface was very limited. However, at first, a similar strategy could not be directly transformed to the gold chip surface, because QCM measurement requires a single layer of F-sugars on the fluorous chip in cm scale with their fluorous tag interacting with the surface and their sugars toward solution, which is crucial to the success of QCM measurement. Inspired by the fluophilic condition for F-SPE, the coating procedure was designed as follows and proved successful. Typically, the gold chip was immersed in the solution of F-sugars (0.2 mg/mL) in MeOH/water = 3:2 (v:v) overnight. Then the chip was washed gently with the mixed solvent and dried. The successful immobilization of F-sugars was characterized by contact angle (Fig. 1c and d), which was measured as 38° ± 3° showing hydrophilicity from the previous hydrophobic fluorous surface.

After F-sugar has been immobilized on the gold chip, QCM measurement was then performed. As shown in Figure 2, after a short wash of HEPES buffer, peanut agglutinin (PNA) solution (0.2 mg/mL, in HEPES buffer) was loaded to the chip immobilized with **F-Lac**. Immediately, a dramatic frequency ($-\Delta F$) increase of the chip was observed within several seconds, indicating the successful absorption of proteins on surface. When $-\Delta F$ reached around 37 Hz, this quick increase reached equilibrium for a short time. Then more proteins were absorbed onto the surface in a slower rate with the total ΔF change less than 5 Hz within 700 s. At the moment, the surface turned to equilibrium again without any increase of $-\Delta F$. Subsequently, PNA in HEPES buffer at a higher concentration (0.5 mg/mL) was flowed to the chip instead of the previous one. After this switch, another 6 Hz increase of $-\Delta F$ was observed within 800 s, which was even much slower to reach

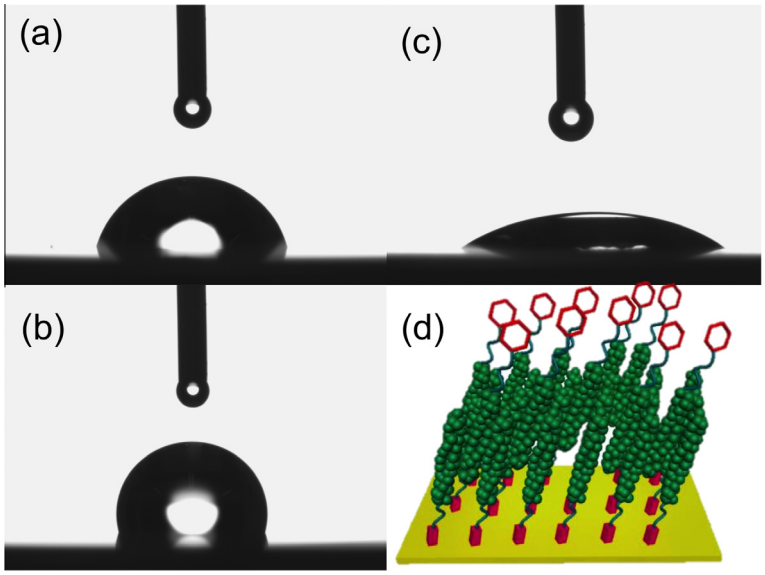

Figure 1. Contact angles of (a) bare gold, (b) fluorous gold surface, (c) after F-sugar coating. (d) Cartoon representation of the gold surface after coating with F-SH and F-sugar.

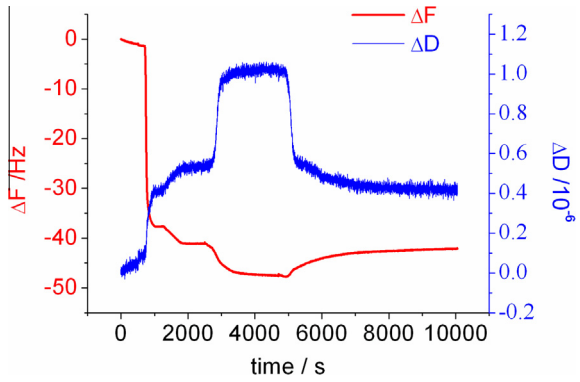

Figure 2. $\Delta F/\Delta D$ responsive curves of the **F-Lac** surface at different PNA concentrations.

"saturation" than the previous one. After the frequency reached equilibrium for a quite long time (3000 s), HEPES buffer was flowed onto the chip in order to remove any non-specific proteins. Slowly the frequency was washed to the equilibrium (42 Hz) before the high concentration of PNA was loaded.

Moreover, by using QCM-D equipped with dissipation, more information could be explored. As shown in Figure 2, ΔD was recorded with frequency as well. When the first equilibrium reached around 1300 s, ΔD increased from 0 to 0.4×10^{-6}, indicating the rigidity of PNA absorbed on surface. As $-\Delta F$ increased again from 1300 s to 2000 s, ΔD increased to 0.6×10^{-6}, following the evolution of $-\Delta F$. After solution concentration of PNA was increased to 0.5 mg/mL, a much more obvious ΔD increase to 1.0×10^{-6} was observed from 2900 s to 3100 s, which reached equilibrium again, following the trend of $-\Delta F$. Importantly, after the surface was washed with HEPES buffer, ΔD returned to the previous value (ca 0.4×10^{-6}). The obvious fluctuation of ΔD showed that the absorption after the concentration of PNA increased to 0.5 mg/mL was quite loose and could be considered as a non-specific interaction, which was different from the PNA absorption at lower concentrations. Similarly, as shown in Figure S1, the absorption of lectin Concanavalin A (Con A) to the surface of **F-Mal** showed two absorption stages with different ΔD and ΔF variations happening as well.

To semi-quantitatively evaluate the binding on surface, continuous concentration variations of lectin were performed. As shown in Figure 3a, when the concentration of PNA was increased step-by-step on **F-Gal** surface, $-\Delta F$ and ΔD increased as well. According to Sauerbrey equation, the mass of absorbed molecules on surface is proportional to ΔF, which can be calculated directly. Then the mass of absorbed PNA *vs* the loaded PNA concentration was drawn in Figure 3, an obvious decrease of the slope was observed when PNA concentration exceeded 0.10 mg/mL, indicating the increase of physical absorbed PNA. A similar experiment of Con A absorbed on **F-Man** surface was also performed, showing similar phenomenon which is presented in Figure S2. According the ΔF data presented in Table 1, apparent binding constant (K_a) was calculated.[10]

After evaluation of carbohydrate–protein interactions on F-sugar surface, another type of interaction participated by sugars, that is, CCI, was also performed. CCI always happens between different glyco-conjugates, for example, short saccharide chains on proteoglycans, as a type of inter-chain interaction, which lacks specific binding sites as those of proteins with less specificity than carbohydrate–protein interaction.[11] Thus CCI was employed as the second model system measured on the fluorous QCM platform. Glyco-nanoparticles (GNPs) with different type of sugars on their surface were employed as models for different glyco-conjugates. The GNPs were prepared according to our previous reported procedure by using triblock copolymers containing conjugated polyfluorine as the middle block and different glycopolymers as side blocks.[12] After self-assembly, the GNPs formed with α-mannopyanoside, α-galactopyranoside, and α-glucopyranoside on the surface, are coded as NP-Man, NP-Gal, and NP-Glu, respectively. Typical frequency response curves are shown in Figure 4. To the **F-Lac** surface (Fig. 4a), NP-Gal bound much stronger than NP-Man and NP-Glu, supported by the much more obvious frequency change ($-\Delta F$ = 120 Hz) of the former than the other two. And NP-Man showed a weak binding with about 28 Hz increase of $-\Delta F$. Interestingly, NP-Glu did not show any obvious binding to the **F-Lac** surface, with the frequency remaining constant. Similarly, on the surface of **F-Man**, different binding effect of GNPs was observed. The $-\Delta F$ increase was following the same sequence on **F-Lac** surface, that is, NP-Gal > NP-Man > NP-Glu. However, the obtained $-\Delta F$ values were much smaller than those of **F-Lac**. As shown in Figure 4b and Table 2, $-\Delta F$ increase of **F-Man** surface

Table 1
Frequency changes of different lectins on different F-sugar surfaces (average value was obtained via experiments repeated for three times)

Surface/lectin	$-\Delta F$/Hz	$-\Delta F_{max}$/Hz	Lectin/μM	K_a/M^{-1}
F-Lac/PNA	43.2 ± 3.5	48.4 ± 3.6	2.0	$4.3 \times 10^6 \pm 0.5 \times 10^6$
F-Mal/ConA	22.2 ± 1.8	28.1 ± 1.3	2.0	$1.8 \times 10^6 \pm 0.2 \times 10^6$
F-Man/ConA	27.5 ± 2.3	38.1 ± 3.4	2.0	$1.3 \times 10^6 \pm 0.7 \times 10^6$
F-Gal/PNA	13.4 ± 2.2	18.8 ± 1.7	2.0	$1.2 \times 10^6 \pm 0.3 \times 10^6$

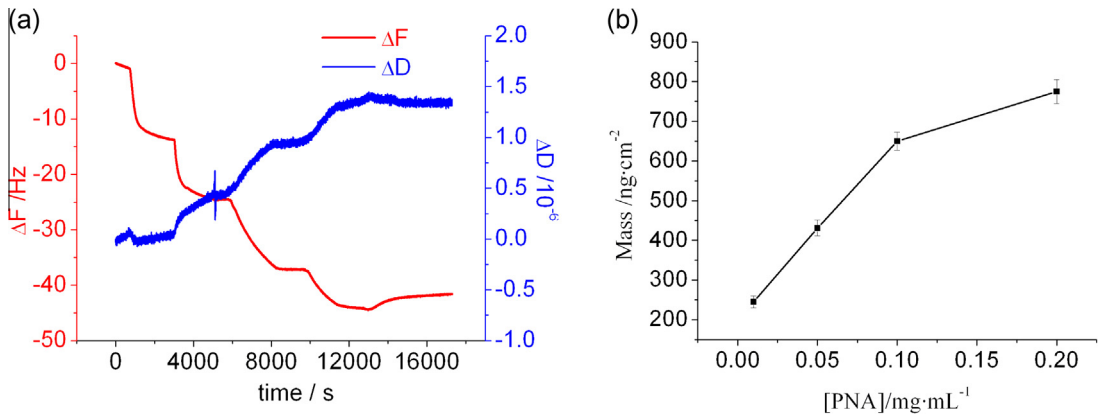

Figure 3. (a) Frequency response curves of the **F-Gal** surface with different PNA concentrations. (b) The linear relationship between frequency response and PNA concentration.

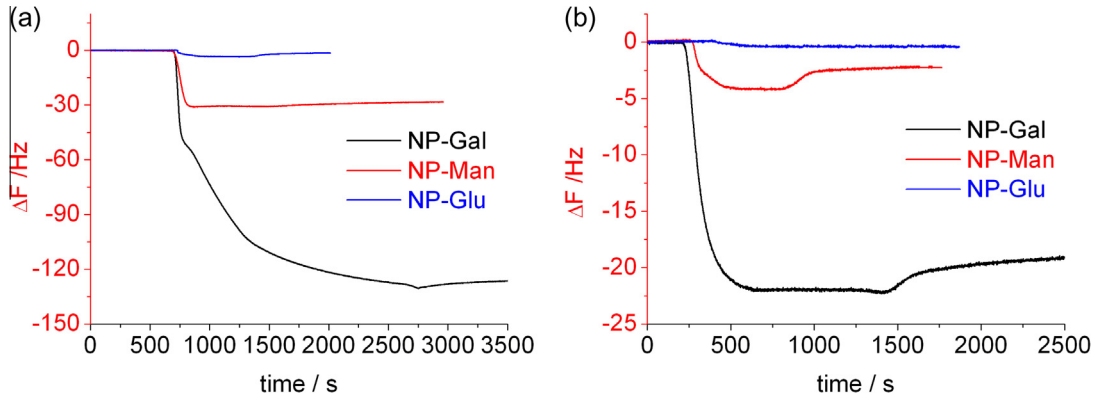

Figure 4. Frequency response curves of the (a) **F-Lac** and (b) **F-Man** surface with different GNPs.

Table 2
Frequency changes of different GNPs on different F-sugar surfaces (average value was obtained via experiments repeated for three times)

GNPs surface	NP-Gal $-\Delta F$/Hz	NP-Man $-\Delta F$/Hz	NP-Glu $-\Delta F$/Hz
F-Lac	120 ± 21	28 ± 5	4 ± 1
F-Mal	45 ± 8	30 ± 4	5 ± 2
F-Gal	20 ± 2	5 ± 2	0 ± 0
F-Man	20 ± 3	5 ± 2	0 ± 0

to NP-Gal was only about 20 Hz, while that of **F-Lac** was 120 Hz. Moreover, for NP-Man, $-\Delta F$ increase of **F-Man** surface was only around 5 Hz, while that of **F-Lac** was about 30 Hz. The binding behavior between different GNPs and F-sugar surfaces was compared as shown in Table 2. On each surface, the interaction of different GNPs is following the sequence of NP-Gal > NP-Man > NP-Glu. To each GNP, **F-Lac** surface shows the most significant increase of $-\Delta F$, while that of **F-Mal** is less but still obvious. However, on **F-Man** and **F-Gal** surfaces, almost no NP-Man and NP-Glu was immobilized, with a minor $-\Delta F$ change less than 5 Hz. In short, two conclusions may be drawn from these results: (a) CCI exists between simple sugars (mono- and di-saccharides), when repeating sugar units are available as pendent groups on polymer chains of GNPs; (b) the strongest interaction between NP-Gal and **F-Lac** could be explained by the hydrophobic interaction of B-faces (hydrophobic surface) existing in galactopyranosides.

Acknowledgments

Ministry of Science and Technology of China (2011CB932503), National Natural Science Foundation of China (Nos. 91227203, 51322306), Innovation Program of Shanghai Municipal Education Commission and the Shanghai Rising-Star Program (Grant 13QA1400600) are acknowledged for their financial supports.

Supplementary data

Supplementary data (synthesis and characterization of **F-Mal**, **F-Lac**, **F-Gal**, **F-Man** including ^{1}H NMR results) associated with this article can be found, in the online version, at http://dx.doi.org/10.1016/j.carres.2014.07.023.

References

1. (a) Gladysz, J. A.; Curran, D. P.; Horváth, I. T. *Handbook of Fluorous Chemistry*; WILEY-VCH, 2004; (b) Curran, D. P. *Science* **2008**, *321*, 1645–1646.
2. Cametti, M.; Crousse, B.; Metrangolo, P.; Milani, R.; Resnati, G. *Chem. Soc. Rev.* **2012**, *41*, 31–42.
3. (a) Zhang, W.; Curran, D. P. *Tetrahedron* **2006**, *62*, 11837–11865; (b) Zhang, W.; Lu, Y. *J. Comb. Chem.* **2006**, *8*, 890–896.
4. (a) Ko, K.-S.; Jaipuri, F. A.; Pohl, N. L. *J. Am. Chem. Soc.* **2005**, *127*, 13162–13163; (b) Chen, G.-S.; Pohl, N. L. *Org. Lett.* **2007**, *10*, 785–788.
5. (a) Nicholson, R. L.; Ladlow, M. L.; Spring, D. R. *Chem. Commun.* **2007**, 3096–3908; (b) Wilson, R. L.; Frisz, J. F.; Hanafin, W. P.; Carpenter, K. J.; Hutcheon, I. D.; Weber, P. K.; Kraft, M. L. *Bioconjugate Chem.* **2012**, *23*, 450–460.
6. (a) Lu, C.; Czanderna, A. W. *Applications of Piezoelectric Quartz Crystal Microbalances*; Elsevier: New York, 1984; (b) Ward, M. D.; Buttry, D. A. *Science* **1990**, *249*, 1000–1007.
7. Ferreira, G. N. M.; da-Silva, A. C.; Tomé, B. *Trends Biotechnol.* **2009**, *12*, 689–697.
8. Rodahl, M.; Höök, F.; Fredriksson, C.; Keller, C. A.; Krozer, A.; Brzezinski, P.; Voinova, M.; Kasemo, B. *Faraday Discuss.* **1997**, *107*, 229–246.
9. Mamidyala, S. K.; Ko, K.-S.; Jaipuri, F. A.; Park, G.; Pohl, N. L. *J. Fluorine Chem.* **2006**, *127*, 571–579.
10. (a) Zhang, Y.; Luo, S.; Tang, Y.; Yu, L.; Hou, K.-Y.; Cheng, J.-P.; Zeng, X.; Wang, P. G. *Anal. Chem.* **2006**, *78*, 2001–2008; (b) Ebara, Y.; Itakura, K.; Okahata, Y. *Langmuir* **1996**, *12*, 5165–5170.
11. (a) Matsuura, K.; Oda, R.; Kitakouji, H.; Kiso, M.; Kitajima, K.; Kobayashi, K. *Biomacromolecules* **2004**, *5*, 937–941; (b) Santacroce, P. V.; Basu, A. *Angew. Chem., Int. Ed.* **2003**, *42*, 95–98.
12. Sun, P.; He, Y.; Lin, M.; Zhao, Y.; Ding, Y.; Chen, G.; Jiang, M. *ACS Macro Lett.* **2014**, *3*, 96–101.